Korean Journal of Remote Sensing, Vol.34, No.1, 2018, pp.45~74
http://dx.doi.org/10.7780/kjrs.2018.34.1.4

ISSN 1225-6161 (Print)
ISSN 2287-9307 (Online)

Article

Data Mining-Aided Automatic Landslide Detection Using Airborne Laser Scanning Data in Densely Forested Tropical Areas

Mustafa Ridha Mezaal*, and Biswajeet Pradhan†**

*Department of Civil Engineering, University Putra Malaysia
**School of Systems, Management and Leadership, Faculty of Engineering and Information Technology, University of Technology Sydney, Australia

Abstract : Landslide is a natural hazard that threats lives and properties in many areas around the world. Landslides are difficult to recognize, particularly in rainforest regions. Thus, an accurate, detailed, and updated inventory map is required for landslide susceptibility, hazard, and risk analyses. The inconsistency in the results obtained using different features selection techniques in the literature has highlighted the importance of evaluating these techniques. Thus, in this study, six techniques of features selection were evaluated. Very-high-resolution LiDAR point clouds and orthophotos were acquired simultaneously in a rainforest area of Cameron Highlands, Malaysia by airborne laser scanning (LiDAR). A fuzzy-based segmentation parameter (FbSP optimizer) was used to optimize the segmentation parameters. Training samples were evaluated using a stratified random sampling method and set to 70% training samples. Two machine-learning algorithms, namely, Support Vector Machine (SVM) and Random Forest (RF), were used to evaluate the performance of each features selection algorithm. The overall accuracies of the SVM and RF models revealed that three of the six algorithms exhibited higher ranks in landslide detection. Results indicated that the classification accuracies of the RF classifier were higher than the SVM classifier using either all features or only the optimal features. The proposed techniques performed well in detecting the landslides in a rainforest area of Malaysia, and these techniques can be easily extended to similar regions.

Key Words : Data Mining, Landslide Detection, LiDAR, Orthophotos, GIS, Remote Sensing

1. Introduction

Landslide is a natural disaster that adversely affects lives and properties (Jebur *et al*., 2014). Therefore, continuously developing detailed and updated landslide inventory maps is important (Lin *et al*., 2013). These maps are important data sources for landslide susceptibility mapping and risk assessment (Ardizzone *et al*., 2007; Fiorucci *et al*., 2011; Guzzetti *et al*., 2012; Van Westen *et al*., 2008). Landslides must be

Received January 3, 2018; Revised February 7, 2018; Accepted February 12, 2018; Published online February 22, 2018
† Corresponding Author: Biswajeet Pradhan (Biswajeet24@gmail.com)

accurately detected to produce high-quality landslide inventory maps (Siyahghalati *et al*., 2016). However, mapping a landslide inventory in tropical areas is challenging because the dense vegetation cover in these regions obscures underlying landforms (Pradhan *et al*., 2016; Chen *et al*., 2015).

Landslide inventory maps are traditionally produced by visually interpreting aerial photographs. This technique inevitably requires several field surveys; thus, it is time-consuming and costly (Van Den Eeckhaut *et al*., 2005). Field mapping may also fail to provide a complete view of large-scale landslides in certain areas, particularly in densely vegetated areas. Old landslides are also sometimes difficult to visualize using aerial photographs or satellite images because of the vegetation cover or the alteration caused by other slope failures and human activities (Miller *et al*., 2012). Consequently, this method enables researchers to map and recognize single and small groups of landslides (Galli *et al*., 2008).

Usually, visual interpretation of aerial photographs is used in the traditional techniques in the construction of landslide inventory maps which requires multiple field surveys. This approach could be quite expensive and time consuming. According to Brardinoni *et al*. (2003) traditional techniques include visual interpretation of stereoscopic aerial photographs and geomorphological field mapping. However, geomorphological field mapping experience certain level of limitations such as degree of landslide which is usually too big to be completely studied in an area. Therefore, research activities are limited in terms of perspective in distinguishing all the features of landslide in detail. (Miller *et al*., 2012) reported that most at times old landslides are usually covered by vegetation or have experienced slope feature changes. Therefore, this method gives investigators avenue to recognize and map single landslide or minor groups of landslides (Galli *et al*., 2008). Lee *et al*. (2012) reported that some of the oldest techniques used for landslide detection are still in use today despite substantial progress made in the technology of aerial photographs. The deployment of vertical exaggeration using stereoscope enables the morphological structure of land to be amplified to ease detection of changes in slopes. According to Nichol *et al*. (2006) this method does not require any sophisticated technical capabilities. Also, Malamud *et al*. (2004) reported that an aerial photograph having fine scale and a large size can cover the entire location of landslide in a particular period. This sets of aerial photographs for similar regions could serve as a valuable resource for research works to conduct a temporal evaluation of landslides (Miller *et al*., 2012). The use of aerial photography in detecting slope failures is an uncertain technique that requires training, an organized methodology, skills and proper interpretation principles (Antonini *et al*., 2002). However, there seems to be no standard procedure yet available to identify and categorize landslide based on the investigation and knowledge of set of features that can be to recognized images (Pradhan *et al*., 2016). Besides, vegetation thickness and height and changes influence the way slope failure are recognized when using aerial photographs (De Blasio, 2011).

Optical remote sensing and synthetic aperture radar (SAR)-based remote sensing have led to significant progress in landslide inventory mapping. Remote sensing data that are useful for landslide studies include SAR images, high-spatial-resolution multispectral images, and digital elevation models (DEMs), which are obtained from space-borne sensors and airborne laser scanning systems (Ardizzone *et al*., 2007; Guzzetti *et al*., 2005; Jebur *et al*., 2014; Stumpf and Kerle, 2011). However, it is difficult to identify landslides in rough topographies and dense vegetation cover using aerial photographs, SAR and VHR and imageries, due to the fact that the morphologic features revealing landslides could be subdued (McKean and Roering, 2004; Wills and McCrink, 2002). Second, data interpretation is frequently based on the expert

knowledge and experience of an analyst as well as his or her familiarity with the area (Chen *et al*., 2014; Malamud *et al*., 2004). Third, additional errors can be introduced while translating image interpretation results into thematic maps (Malamud *et al*., 2004). High-resolution LiDAR-derived DEMs can depict ground surfaces and provide valuable information about the topographic features of possible landslide-affected areas that are covered by dense vegetation (McKean and Roering, 2004). LiDAR technology is considered an effective tool for detecting landslides and mapping the features of densely vegetated areas because of its capability of obtaining high-resolution topographic data by penetrating through the canopy and thick vegetation (Van Westen *et al*., 2008; Borkowski *et al*., 2011; Pradhan *et al*., 2016; Wang *et al*., 2013). LiDAR data and their derivatives, such as hillshade, surface roughness, slope, and contour maps, provide significant and valuable information about active geological processes, such as landslides, which reshape the topography of an area (Booth *et al*., 2009; McKean and Roering, 2004; Van Den Eeckhaut *et al*., 2011).

In the area of remote sensing and geoscience, image analysis methods are commonly used in studying landslide. According to Gao and Mas(2008), pixel-based and object-based image analysis (OBIA) methods have been Compared in numerous studies. OBIA can be applied at different scales, unlike the pixel-based analysis (PBA). Various objects sizes that depict different land features can be produced depending on the selected application such as environment under analysis and underlying input imagery. OBIA can develop contextual semantic features and additional geometry that can be used for classification studies (Duro *et al*., 2012). In heavily forested areas, OBIA using LiDAR data have evolved to be an alternative approach due the difficulty in the use of optical image-based analysis vegetated in rugged and terrain (Li *et al*., 2016). Conversely, the pixel-based approach (Fei and Lee, 2009; Rau *et al*., 2012) usually create pepper-and-salt effect that makes onsite identification difficult with poor transferability (Drăguţ and Blaschke, 2006).

A sufficient number of training areas should be used to represent the variability of a class (Pal and Mather, 2003). Furthermore, time and cost efficiency should be considered when designing a sampling scheme to achieve high accuracy (Lippitt *et al*., 2008). An adequate training set size is needed to obtain high classification accuracy (Foody and Mathur, 2006; Pal and Mather, 2003). Most of the cited studies used a random sampling method to obtain the reference data for training and assessment (Puissant *et al*., 2014; Zhen *et al*., 2013). However, this sampling method is not always suitable because it leans toward under-sampling, but increasing the training set size is imperative for mapping categories.

Feature subset selection is crucial in data mining (Karegowda *et al*., 2010). The high-dimensional dataset, however, makes it difficult for testing and training the classification methods. Few object-based studies have handled the features selection for landslide detection by using LiDAR data (Chen *et al*., 2014; Li *et al*., 2015). Karegowda *et al*.(2010) demonstrated the significance of features selection by using Correlation-based Feature Selection (CFS) and gain ratio algorithms. Aladesote *et al*.(2016) applied two feature selection techniques, namely, Gain Ratio Feature (GR) selection and principal component analysis (PCA) to an intrusion detection system. Their results indicated that both algorithms efficiently selected highly relevant features from a dataset. Chen *et al*.(2014) successfully applied RF for feature selection. Venkateswaran *et al*.(2016) compared Particle Swarm Optimization (PSO) and Genetic Algorithm (GA) and found that the former was effective on LISSIV Madurai imagery and more accurate than the GA. Dou *et al*. (2015) proposed an automatic landslide detection method using an integrated approach consisting of object-oriented image analysis, a GA, and a case-based reasoning technique.

They found that the GA was the best algorithm. Imani *et al*. (2012) integrated GA and Ant Colony Optimization (ACO), and the integrated model presented better performance than the standard GA and ACO did. However, Dadaneh *et al*.(2016) applied ACO to feature selection and asserted the effectiveness of ACO; However, they did not use a LiDAR intensity data. For object based image analysis (OBIA), optimizing multiresolution segmentation parameters for landslides plays a key role in exploiting the spectral and spatial information. In OBIA, feature selection is considered as a significant step because it improves the performance of the classifier and reduces the complexity of the computation by removing redundant information (Pedergnana *et al*., 2013). In this regard, few studies have examined feature selection algorithm for landslide detection through an object-based approach and only LiDAR data. Therefore, this study aims to optimize multiresolution segmentation parameters by using FbSP optimizer and evaluated six feature selection algorithms in order to find the best combination subset for detection landslide.

This study aimed to investigate suitable algorithms for selecting features in landslide detection using airborne laser scanning data. The specific objectives were as follows: 1) to optimize the multiresolution segmentation parameters, 2) to evaluate the six feature selection algorithms for landslide detection, and 3) to determine the appropriate algorithms for selecting features by using RF and SVM classifiers. The studied algorithms have not been tested in existing former studies, particularly in landslide detection. Selecting the suitable algorithm for landslide detection could improve the accuracy of results.

2. Study Area

The Cameron Highlands is a rainforest area characterized by a dense vegetation cover and frequent occurrences of landslides. The study region covers an area of 26.7 km^2. Geographically, the Cameron Highlands is located in the north of peninsular Malaysia at a latitude range of 4°24′32″N–4°24′43″N and a

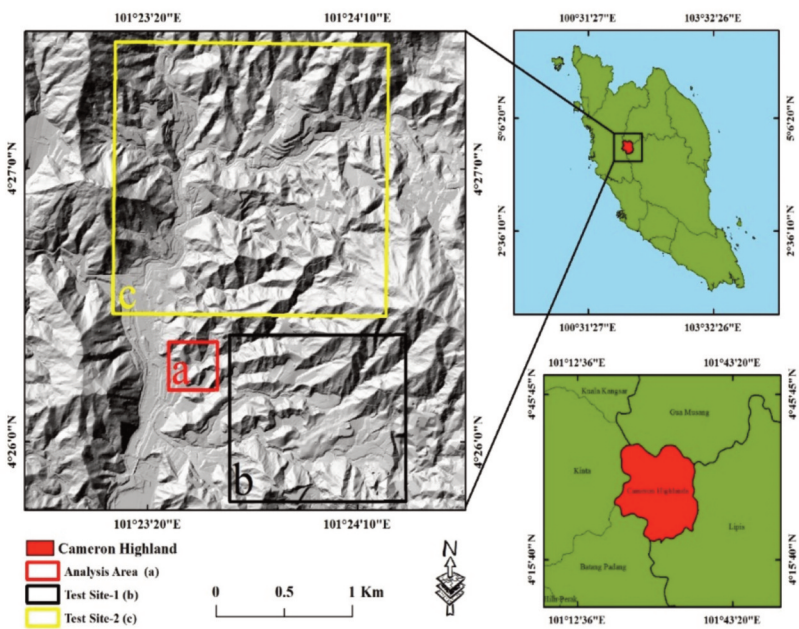

Fig. 1. Shows study is that consist of [red] Analysis area; [black] Test site-1; and [yellow] Test site-2.

longitude range of 101°22′54″E–101°23′11″E. The annual average rainfall in the area is approximately 2,660 mm. Its average temperature is approximately 24°C and 14°C during daytime and nighttime, respectively. A large part of the area (approximately 80%) is forested, and the slope inclination in the area range from flat terrain (0°) to hilly area (80°). Three sites were selected for the analysis of the proposed method, as shown in Fig. 1. These sites were selected according to information obtained from an inventory map. The site (a) was used for developing the method of landslide detection, whereas sites (b) and (c) were used for testing the method in terms of model transferability. Considerations were taken into account in selecting the sites to avoid the missing in land-cover classes.

3. Methodology

According to Lu and Wong (2008), digital surface model (DSM), digital elevation model (0.5 m) (DEM), and intensity feature are produced by converting LiDAR point cloud into raster data through inverse distance weighting (IDW) interpolation. DEM is then used to generate other LiDAR-derived products (i.e., slope, aspect, hillshade). Subsequently, normalized digital surface model (nDSM) also known as Height were produced by subtracting the DSM from DEM. Then, the LiDAR-derived products and orthophotos were combined by correcting their geometric distortions, integrating them into a coordinate system, and then prepared in a GIS for feature extraction. Next, the FbSP optimizer developed by Zhang *et al*. (2010) was used to acquire the suitable parameters (scale,

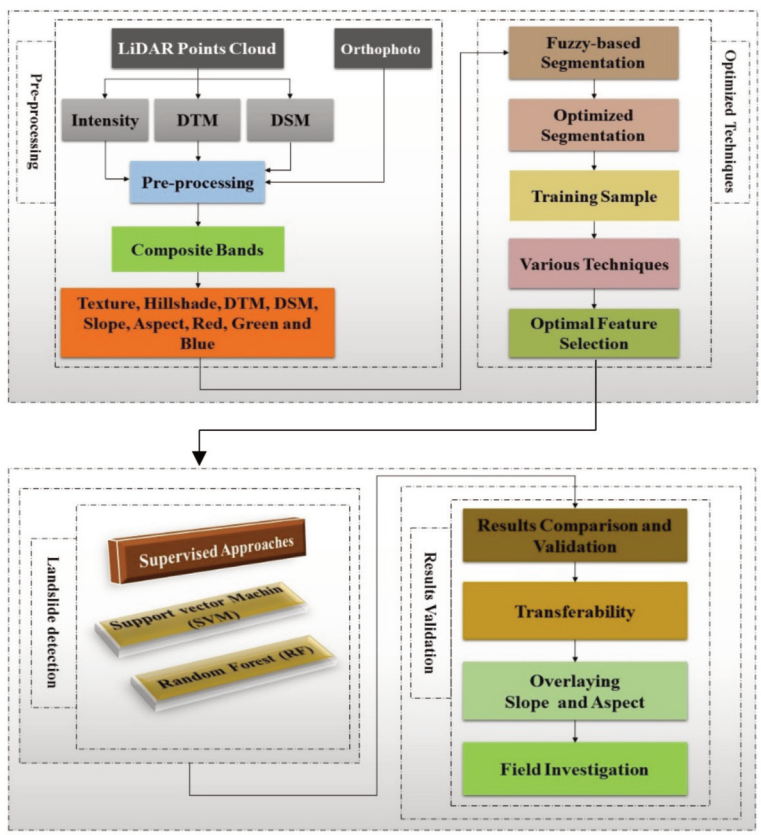

Fig. 2. Flow chart of processing steps that were followed in the current study.

shape, and compactness) at different segmentation levels. Subsequently, the training samples were evaluated using a stratified random scheme following the procedure adopted by Ma *et al*. (2016). Relevant features were selected using the six algorithms and ranked from the most important. Two supervised learning models, namely, SVM and RF, were used to identify the locations of the landslides. The transferability of each classifier model was then verified by applying it to other sites (i.e., Test site-1 and Test site-2). Finally, the results were validated and compared using a confusion matrix and overlaid with the slope and aspect derived from the LiDAR DEM data to identify other characteristics of the landslide, such as direction, runoff, width, and length. The flowchart of the proposed method is illustrated in Fig. 2.

1) Data Used

The LiDAR point cloud data were collected in an area of 26.7 km^2 over the Ringlet and surrounding area of the Cameron Highlands at a flying height of 1510 m. The LiDAR data and were captured on January 15, 2015. The point density was 8 points per square meter and the pulse rate frequency was 25,000 Hz. The absolute accuracy of the LiDAR data should meet the root-mean-square errors of 0.15 m in the vertical axis and 0.3 m in the horizontal axis as standardized by Department of Survey and Mapping Malaysia (JUPEM). The same system for the collection of LiDAR point cloud data in the study area was used to collect the orthophotos. A DEM with 0.5 m spatial resolution was interpolated from the LiDAR point clouds after the non-ground points were removed using inverse distance weighting, with GDM2000/ Peninsula RSO as the spatial reference.

Subsequently, the LiDAR-based DEM was used in generating a number of derived layers to facilitate the detection of landslides and their characteristics (Miner *et al*., 2010). The slope is considered an important factor of land stability because of its direct impact on landslide phenomenology (Martha *et al*., 2011). Moreover, the slope is the principal factor affecting the landslide occurrences (Pradhan and Lee, 2010). Hillshade map provides a good image showing terrain movement, and this map facilitates landslide mapping (Olaya, 2009). The accuracy of a DEM accuracy and its capability to represent the surface are affected not only by terrain morphology and sampling density but also by the interpolation algorithm (Barbarella *et al*., 2013). In the current study, hillshade, intensity, height (nDSM), slope, and aspect were derived from the LiDAR-based DEM, orthophotos, and texture information were utilized for detecting landslides, as shown in Fig. 3.

2) Image Segmentation

is the initial and prerequisite step in object-based analyses because it determines the sizes and shapes of image objects (Duro *et al*., 2012). The selection of the appropriate parameters of image segmentation relies on the selected application, the environment under analysis, and underlying input imagery (Blaschke *et al*., 2010). Multiresolution segmentation is a bottom-up region-merging technique that merges the most similar adjacent regions as long as the internal heterogeneity of the resulting object does not exceed the user-defined threshold of the scale factor (Benz *et al*., 2004). The multiresolution segmentation was carried out on the basis of color, scale and shape including compactness and smoothness of the shape using the eCognition software (Definiens *et al*., 2007). Considering the complex characteristics of landslides such as variations in land cover, differences in illumination, diversity of spectral behavior, and size variability, it is difficult to delineate each individual landslide as a single object (Martha *et al*., 2010).

Three parameters (i.e., scale, shape, and compactness) should be identified in this algorithm. The values of these parameters can be determined using the traditional trial-and-error method, which consumes considerable

time and demands extensive work (Pradhan *et al*., 2016). Therefore, various automatic and semiautomatic methods for identifying the optimal parameters have been explored (Sameen and Pradhan, 2017; Martha *et al*., 2011; Anders *et al*., 2011; Belgiu and Drăguţ, 2014; Drăguţ *et al*., 2010). The Taguchi optimization method proposed by Pradhan *et al*. (2016) and the fuzzy logic supervised approach (i.e. Fuzzy-based Segmentation Parameter optimizer (FbSP optimizer) presented by Zhang *et al*. (2010) are among the advanced methods for the automatic selection of segmentation parameters. Nevertheless, delineating image objects at various scales remains a challenge. Furthermore, not all selected features are completely exploited using a particular segmentation scale. Accordingly, an automatic method should be directly implemented.

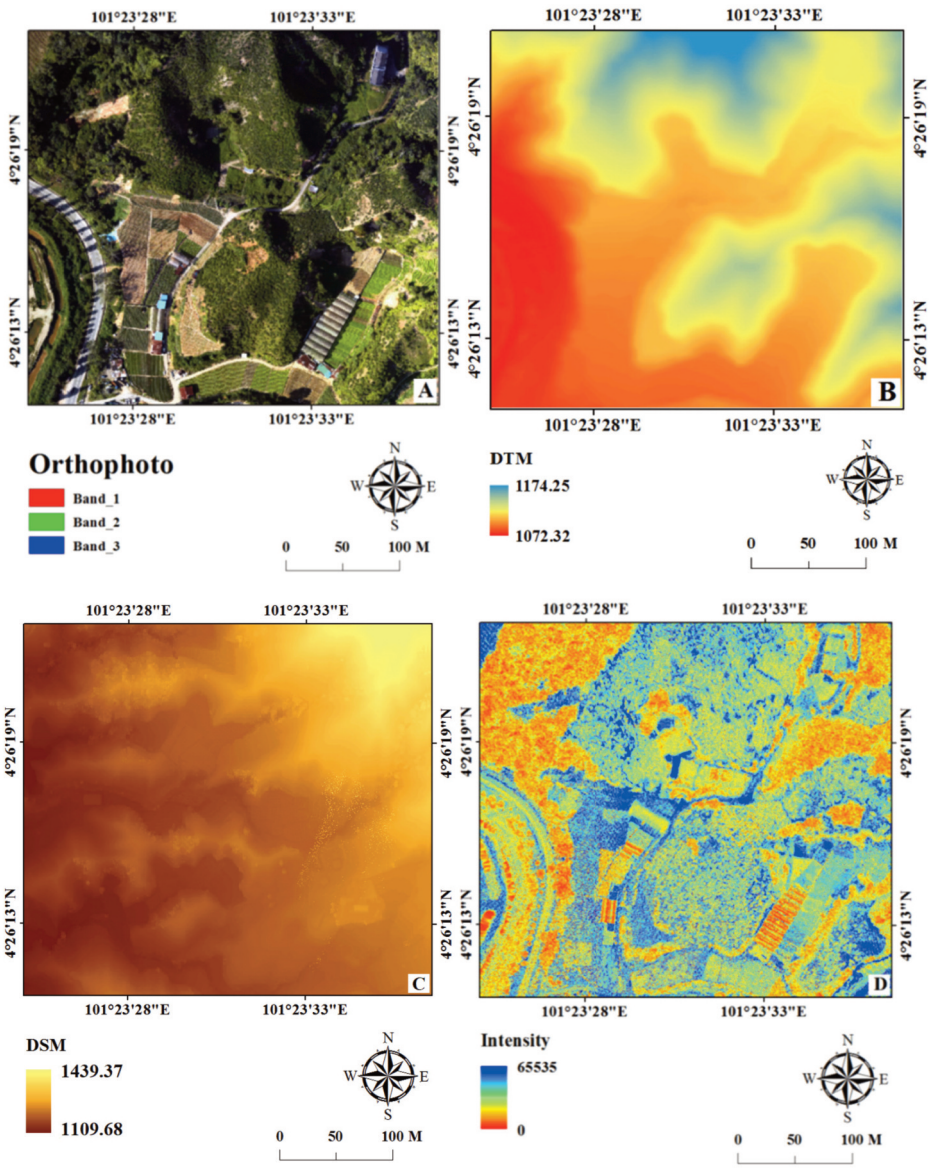

Fig. 3. Shows LiDAR derived data (A) Orthophotos (B) DTM (C) DSM (D) Intensity (E) Height (F) Slope (G) Aspect.

3) Generating Training Datasets

According to Ma *et al*. (2016), landslide inventory should be used to obtain prior knowledge of all the sites, and this step is a prerequisite in the stratified random sampling method. Thus, in this present study, the segmentation scale was optimized, and the landslide inventory map was overlapped with the segmented layer in order to label the classes. The sample sets were constructed automatically at optimal scale of the analysis area by using ArcGIS 10.3 software. Subsequently, stratified random sampling was implemented on the labeled objects. This process was conducted and repeated 20 times at optimal scale. In this study, the training sets were evaluated, a training set with 70% of the training samples (i.e., 30% testing set). Stratified random sampling is recommended to acquire an adequate training set size for every class

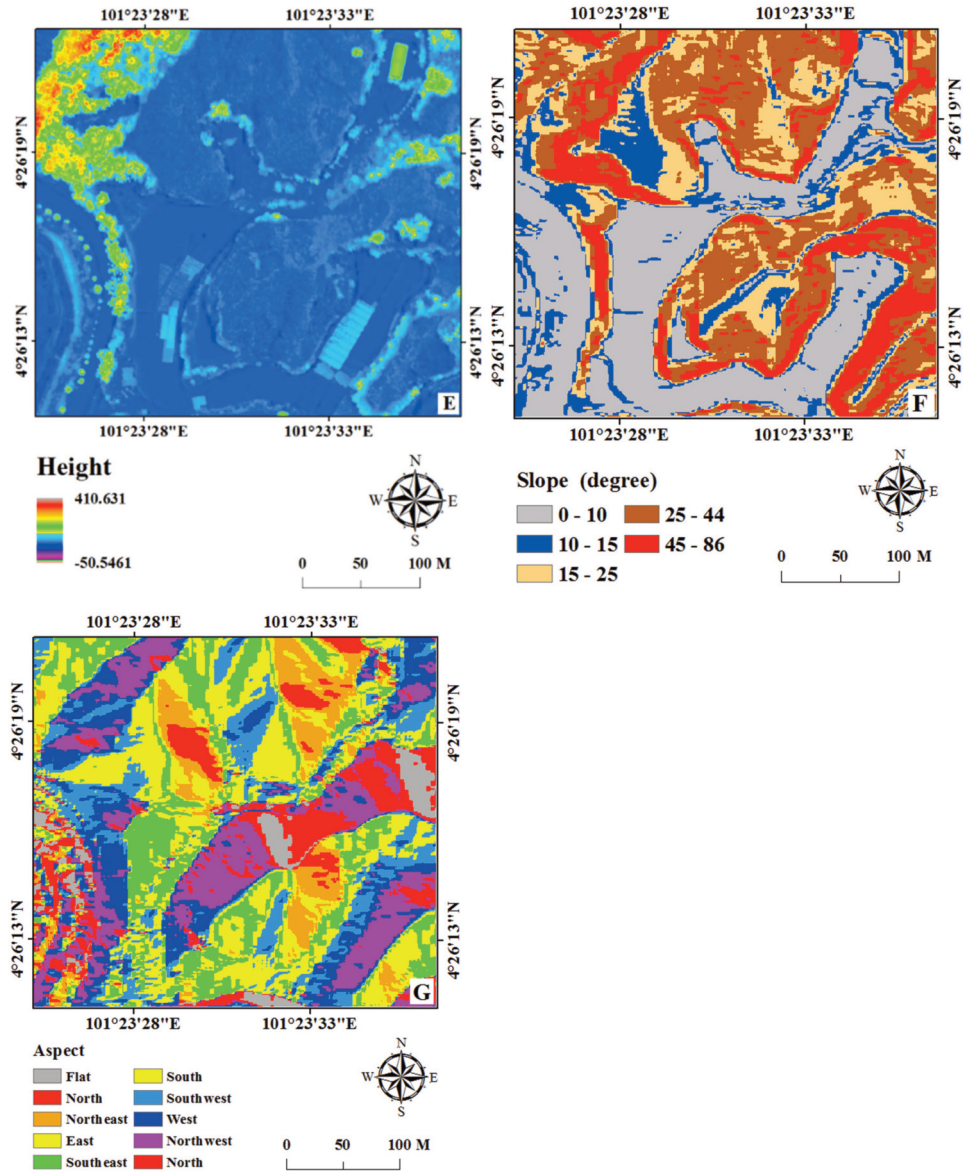

Fig. 3. Continued

without any bias during sample selection (Ma *et al*., 2016). Therefore, this sampling model was adopted in this study to evaluate the training samples and achieve improved results without strong bias.

4) Image Analysis Approaches.

According to Li *et al*. (2016), Support Vector Machines (SVM) and Random Forest (RF) are suitable for object-based techniques. Hence, the tendency of the overall accuracies declining with increase segmentation scale is confirmed. Therefore, SVM and RF classifiers were used for evaluating performance of six feature selection methods.

(1) SVM Model

A supervised non-parametric statistical learning technique was used to categorize the data set into groups in the manner consistent with training examples. SVMs are gaining popularity in the remote sensing field, including landslide mapping (Heleno *et al*., 2015; Van den Eeckhaut *et al*., 2012; Chang *et al*., 2012; Moosavi *et al*., 2014), due to their ability to handle data with unknown statistical distributions and small training data sets as obtainable in the field (Mountrakis *et al*., 2011). Dou *et al*. (2015) found that SVMs with a small training dataset was more accurate and stable than the maximum likelihood, decision tree, and artificial neural network classifiers with large training data sets. SVMs are binary classifiers whose aim is to find the decision region boundary that separates the data set characteristics or features into two regions in the feature space. The SVM chooses the boundary optimal hyperplane that exhibits the maximum safety margin to the closest training features refer to as support vectors which maximizes the margin between the classes (Heleno *et al*., 2016). The linearization of the decision boundary was achieved through the use of kernel functions that maps the training data into higher-dimensional space capable of linearly separating the two classes of hyperplane (Pawłuszek and Borkowski, 2016). The SVMs perform a nonlinear transformation of covariates into high-dimensional feature space (Pradhan and Lee, 2010). In case of linear data separation, a separating hyperplane could be defined as follows (Eq. 1):

$$y_i\,(w.x_i + b) \geq 1 - \delta_i \tag{1}$$

where w is a coefficient vector which determines the orientation of the hyperplane in the feature space and b is the offset of variables (Cortes and Vapnik, 1995), x_i is the input vector, y_i is the desired output. The. In order to determine the optimal hyperplane, the Lagrangian multipliers must first be solved (Samui, 2008) (Eq. 2 and Eq. 3).

$$minimize \sum_{i=1}^{n} \alpha_i - \frac{1}{2}\sum_{i=1}^{n}\sum_{i=1}^{n} \alpha_i\,\alpha_j\,y_i\,y_j\,(x_i x_j) \tag{2}$$

$$subjected\ to \sum_{i=1}^{N} \alpha_i\,y_j = 0,\ 0 \leq \alpha_j \leq C \tag{3}$$

where a_i are Lagrange multipliers, C denotes the penalty, and the slack variables δ_i allow violation of the penalized constraint. The decision function, which is used to classify new data, is illustrated in Equation 4.

$$g(x)\ sign\left(\sum_{i=1}^{N} y_i\,\alpha_i\,x_j + b\right) \tag{4}$$

In some cases, determining the separating hyperplane is impossible through the four available basic kernel – linear (LF), polynomial (PF), radial basis (RBF), and sigmoid (SF) functions. LF is the simplest one; PF is non-stationary and well suited when all training data are normalized; SF is from the field of neural networks; and RBF depends on the distance from the origin as shown in Eq. 5.

$$K(x_i, x_j) = \exp(-\gamma \parallel x_i, x_i \parallel^2),\ \gamma > 0 \tag{5}$$

In this study, SVM was implemented using e1071 package Meyer *et al*. (2014) within the R statistical computing software (RDevelopment CORE TEAM, 2010). The performance of a SVM classifier depends on its hyperparameters. Therefore, selection of these parameter was optimized and their sensitivity was

analyzed. In the case of SVM, three parameters were evaluated namely kernel function, penalty parameter (C) and gamma parameter (γ). The best prediction accuracy was achieved with the Radial basis function (RBF), using Gamma parameter (γ) 0.9 and penalty parameter of 300. This was carried out in an expedite manner, by visual inspection of the match between results and reference data. The 70% of the inventory map together with all the features were selected as training sets to train the RF model.

(2) RF Model

The RF algorithm developed by Breiman *et al*. (2001) is a nonparametric ensemble learning method based on several decision trees for classification or regression. This supervised method has been successfully applied in the detecting landslide using various *types of remote sensing data* (Chen *et al*., 2017; Chen *et al*., 2014; Stumpf and Kerle, 2011). The algorithm constructs multiple decision trees based on randomly selected subsets of the training dataset. In a classification problem, the RF exploits the high variance among individual trees. It assigns the respective class according to the majority votes. The main advantage of this method is the reasonable performance on complex datasets with less efforts of fine-tuning (Stumpf and Kerle, 2011). A RF is considered a random subset of the original set of features, whereas a classification and regression tree considers all variables in each node. Users can estimate the number of variables per node by using the square root of the total variable number. Two mechanisms, namely, sampling and using random variables in each node, generate significantly different uncorrelated trees. Moreover, having a relatively large number of trees is necessary to derive the variability of the training data and achieve high-accuracy classification. A feature is assigned to a class by considering the votes of all the trees in the forest. The class will then be assigned on the basis of the majority vote. (see Eq.6).

$$cT\sqrt{MNlogN}, \tag{6}$$

where c is a constant dependent of data complexity (i.e., small or large dataset), T is the number of tree, M is the number of variables, and N is the number of instances (Breiman, 2003).

In this study, the RF package (Liaw and Wiener, 2002) an open-source statistical language R (R Development Core Team 2013) was used. Two parameters were used: the number of variables in the random subset at each node and the number of trees in the forest. The number (500) was selected for trees in this study which is usually used for the RF classifier as reported by Stumpf and Kerle (2011), while one randomly split variable was used to make the trees grow. The 70% and 30% were used for the inventory map together with all the features as training sets to train the RF model and evaluation of the classification accuracies respectively. The mean and stdev values of the classification accuracies were then drawn from 50 random runs.

5) Features Selection

Feature selection methods are divided into a filter, wrapper, and embedded methods (Ladha and Deepa, 2011). The first method is suboptimal and independent of the classification algorithm, and this method requires less computation for a large dataset (Ladha and Deepa, 2011). The second method measures the feature set using the classification method itself; thus, the selected features depend on the classifier model used. This method is time-consuming and complex because each considered feature should be evaluated with the classifier algorithm used (Saeys *et al*., 2007). The performance of embedded method declines as the number of introduced irrelevant features increases. Compared with the wrapper method, this method depends on the classifier algorithm and requires short computational time, and it is relatively robust against overfitting (Srivastava *et al*., 2014). Feature selection

algorithms can effectively reduce the number of features and enhance the accuracy of results (Li *et al*., 2015). Handling a large number of features is undesirable because the irrelevant input features may lead to overfitting (Chen *et al*., 2014). By contrast, the selection of a small (possibly minimal) feature set leads to the best possible classification results (Kursa and Rudnicki, 2010). Significant features should be selected to improve the results of landslide detection in a certain area (Kursa and Rudnicki, 2010). Van Westen *et al*. (2008) asserted that selecting relevant features is important in distinguishing landslides from non-landslides and classifying landslides. Stumpf and Kerle (2011) reported that the results obtained after reducing features present improved accuracy. Numerous studies (Borghuis *et al*., 2007; Chen *et al*., 2014; Danneels *et al*., 2007; Moine *et al*., 2009) have examined different feature selection techniques for landslide detection. The results of these studies revealed that valuable information could be obtained using relevant features.

(1) ACO

The ACO is a powerful metaheuristic and optimization technique used for parameter optimization due to its ability to eliminate influence of expert subjectivity. It superior performance can be attributed to its parameters

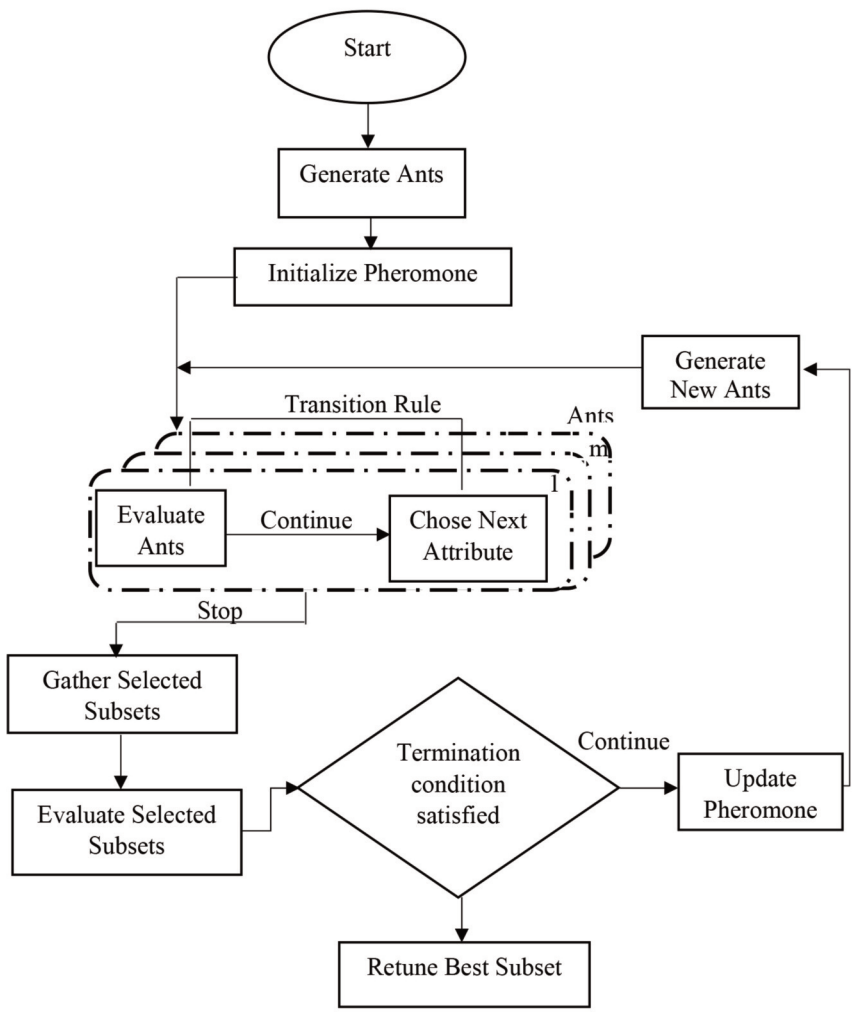

Fig. 4. ACO-based attribute selection workflow.

such as mutation, crossover and survival of chromosomes. Also, derivative information and step size calculation are not necessary in ACO (Ladha and Deepa, 2011). (Dorigo and Stützle, 2003) reported that pheromone evaporation aids in the prevention of rapid convergence of the algorithm toward a suboptimal region. It can perform robust and flexible search for a good combination of terms involving values of the predictor attributes (Parpinelli *et al*., 2002). This approach has been applied conveniently in many remote sensing applications like parameter selection (Alwan and Ku-Mahamud, 2012), feature extraction (Li *et al*., 2012), feature selection (Sameen *et al*., 2017) and image segmentation (Cao and Xia, 2007).

The overall workflow of ACO-based feature selection is presented in Fig. 4 and the process begins with the generation of a number of ants, which are then placed randomly on a graph, i.e., each ant starts with one random attribute. The number of ants located on the graph may be set equal to the number of attributes within the data in which each ant initiates path construction at a different attribute. From their initial positions, the ants traverse nodes probabilistically until a traversal stopping criterion is satisfied and resulting subsets are collected and evaluated. If an optimal subset is found in certain number of times, the process stops, and the best attribute subset encountered is outputted. If none of these conditions hold, the pheromone is updated and a new set of ants is created and the process is reiterated.

(2) GR

The gain ratio is an extension of the information gain measure, which attempts to overcome the bias that the information gain measure is prone to selecting features with a large number of values (Han *et al*., 2011). Thereby, the information gain measure is used as an attribute selection measure of the decision tree and is obtained by computing the difference between the expected information requirement, classifying a tuple in tuples, and the new information requirement for attribute *A* after the partitioning. The measure of the expected information requirement is given by (Han *et al*., 2011) (Eq.7).

$$Info(D) = -\sum_{i=1}^{m} p_i \, i \, log_2(p_i) \tag{7}$$

where *m* is the number of distinct classes; *pi* indicates the probability by calculating the proportion of belonging to class *Ci* in tuples *D*. The new information requirement for attribute A is measured by (Eq. 8).

$$Info(D) = -\sum_{j=1}^{v} \frac{|D_i|}{|D|} \times Info(D_i) \tag{8}$$

where *v* indicates that *D* was divided into *v* partitions or subsets, {D1, D2, …, Dv}. Thus, the information gain measure *Gain*(*A*) for attribute *A* can be calculated by the formula (Eq. 9).

$$Gain(A) = Info(D) - Info_A(\mathrm{D}) \tag{9}$$

Then, a 'split information' function was used to normalize the information gain measure Gain (A). The split information function was defined by (Eq. 10).

$$SpliteInfo_A(D) = -\sum_{j=1}^{v} \frac{|D_i|}{|D|} \times log_2\left(\frac{|D_i|}{|D|}\right) \tag{10}$$

Finally, the gain ratio is calculated as the information gain measure *Gain*(*A*) divided by the split information measure *SpliteInfo*(*A*), as shown in (Eq. 11).

$$GainRatio(A) = \frac{Gain(A)}{SpliteInfo_A(D)} \tag{11}$$

The larger the gain ratio obtained, the more important the represented features are.

(3) PSO

In 1995, Kennedy and Eberhart proposed PSO as a technique which was motivated by social behavior like fish schooling and birds flocking. PSO relies on optimization through social interaction in a population which depends on personal and social behavior. The useful features from the available features of eCognition software were selected using PSO optimization implemented in MATLAB which was used to minimize the error rate. The fitness function is given in (Eq. 12) which is used to minimize the

classification error rate obtained by the selected features during the evolutionary training process and the number of selected features (Xue *et al*., 2013; Sameen and Pradhan, 2017).

$$F = \begin{cases} w \times Train_{ER_s} + (1-w) \times Train_{ER_s} \\ \times \dfrac{\#Feature}{\#All\ Features} + (1-\alpha) \times \dfrac{ER_s}{ER_{all}} \end{cases} \quad (12)$$

where w is the weight of the classification error rate obtained from the training data and $w \in [0,1]$, $Train_{ER_s}$ represents the classification error rate gotten from the selected feature subset and the training subset data, $Test_{ER_s}$ denotes the classification error rate obtained from the selected feature subset and the testing subset data, α is the weight of the number of selected features, #Features represents the number of selected features, #All Features represents the total number of features available for classification, ER_s is the classification error rate obtained from the selected features, and ER_{all} is the classification error rate obtained from all the available features. The error rate of the classification results are calculated from (Eq.13) (Sheikhpour *et al*., 2016), as follows:

$$Error\ Rate\ (ER) = \frac{FP + FN}{TP + TN + FP + FN} \quad (13)$$

where *TP*, *TN*, *FP*, and *FN* represent true positives, true negatives, false positives, and false negatives, respectively.

(4) GA

Goldberg (1989) defined GA as a stochastic class search and optimization techniques based on evolutionary principles and natural selection. When using GA for feature optimization, the feature attributes are coded as chromosomes in a type of binary string. The populations are initially randomized before the search process commence and the searched would then determine the encoded chromosomes to take full advantage of the optimal fitness function, which was computed for each of the randomly originated chromosomes. Because designing, the optimal fitness function remains a key player in improving efficiency of the search space. If improper fitness function are selected in a local optimum, it can lead to decrease the search effectiveness (Tang *et al*., 2005). The fitness function $f(x)$ can be expressed as shown in (Eq. 14 and Eq. 15) which facilitates the assigning of optimal fitness value for each chromosome.

$$f(x) \frac{\sum_{i=1}^{n} \sum_{j=1(\omega_i = \omega_j)}^{n} \delta(x_i, x_i)}{\sum_{i=1}^{n} \sum_{j=1(\omega_i \neq \omega_j)}^{n} \delta(x_i, x_i)} \quad (14)$$

$$\delta(x^i, x^i) = \sqrt{\sum_{k=1}^{n} \omega_k \ (x_k^j - x_k^i)} \quad (15)$$

where x^i represents an n-dimensional feature vector of image object i, $x^i = x_1^i, x_2^i, \ldots, x_n^i$ and $\delta(x^i, x^j)$ represents the Euclidean distance between vectors x^i and x_k^i, which is *k-th* feature value of the i, ω_k is the weight of the *k-th* feature, and n is the number of objects in feature optimization. GA optimization was carried out using MATLAB software and are used to compute the optimal fitness value of each individual and only the optimal individuals survives under this condition. Therefore, an optimized generation process can be used to reproduce generations through crossover or mutation. Eventually, to passage a discrimination related to the fitness, the optimal individuals were decoded for use and corresponded to feature selection as inputs for landside detection and classification in the CBR process.

(5) CFS

The feature subset was evaluated using filter algorithm unlike the feature evaluation methods aforementioned which is a correlation-based Feature Selection (CFS). The CFS measured the worth of a set of features using a heuristic evaluation function based on the correlation of features which is consistent with assertion by Hall and Holmes (2003) who reported that a superior subset of features should be correlated with classes highly uncorrelated to each other. Thus, the criterion of a subset can be evaluated using (Eq. 16).

$$r_{cz} = \frac{Kr_{zi}}{\sqrt{K + K(K-1)r_{ii}}} \quad (16)$$

where r_{zc} represents the correlation between the summed feature subsets and the class variable, k is the number of subset features, r_{zi} is the average of the correlations between the subset features the class variable, and r_{ii} is the average inter-correlation between subset features. In addition, the best first search was used to explore the feature space, and the five consecutive fully expanded non-improving subsets were set to a stopping criterion to avoid searching the entire feature subset space. In this study, the WEKA package was used to implement this feature selection algorithm.

(6) RF

The feature evaluation method was based on random forest known as an embedded method (Pal and Foody, 2010) which provides a variable importance criterion for each feature by computing the mean decrease in the classification accuracy for the out of bag (OOB) data of the bootstrap sampling (Verikas and Gelzinis, 2011). Assuming bootstrap samples $b = 1, \ldots, B$, the mean decrease in classification accuracy D_j for variable x_j as the importance measure is given in (Eq. 17).

$$D_j = \frac{1}{B}\sum_{b=1}^{B}(R_b^{OOb} - R_{bj}^{OOb}) \quad (17)$$

where R_b^{OOb} denotes the classification accuracy of OOB data l_b^{OOb} using the classification model T_j; and R_b^{OOb} is the classification accuracy of OOB data R_b^{OOb} permuted the values of variable x_j in l_b^{OOb} ($j = 1, \ldots, N$). Finally, a z-score of variable x_j representing the variable importance criterion could be computed using the formula $z_j = \frac{D_j}{S_j\sqrt{B}}$, after the standard deviation s_j of the classification accuracy decrease is calculated. In this study, the feature evaluation procedure was performed automatically using the R package 'RRF'.

4. Results of Proposed Methodology

1) Optimizing Segmentation using Supervised Approach

Supervised approach (i.e. Fuzzy-based Segmentation Parameter optimizer (FbSP optimizer) was used to optimize the parameters like shape, scale and compactness of the multiresolution segmentation

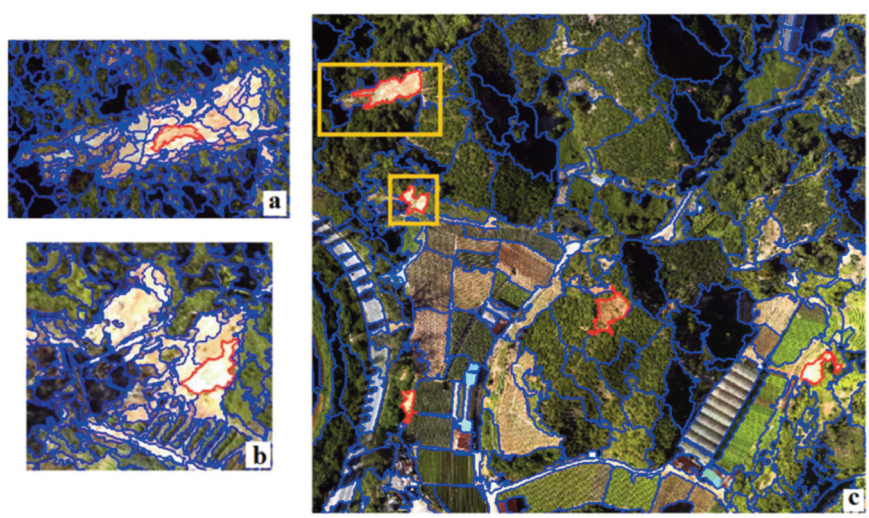

Fig. 5. Shows the result of the segmentation using optimized parameters for the analysis area. It can be seen that the landslide objects were accurately delineated highlighted by red color.

algorithm shape, and compactness, respectively in the analysis area (Fig. 5(a) and (b)). These parameters were visually assessed to achieve an over segmentation. After a few iterations with these initial values, the optimal values obtained for scale, shape, and compactness were 65.37, 0.34, and 0.58, respectively (Fig. 5(c)).

According to the various man-made and natural objects found in the scene such as landslide, cut slope, trees, and bare land, three segmentation levels were found to be necessary. In each class, there are also several types of the same object, which suggested using different levels of segmentation. For example, the cut slope class which represents the previously landslides that maintained by slope engineers have different sizes according to the type and size of the landslide occurred.

The supervised approach presents more significant improvement in terms of time used for the segmentation. It only requires few minutes to achieve optimal segmentation parameters for the landslide segmentation as demonstrated in Fig. 4 which shows improvement in terms of speed. The optimized parameters allowed increasing the overall classification accuracy of delineating the landslide boundaries. As the boundary of the objects could be accurately delineated, the computation and utilization of spatial and textural of the image objects were improved.

2) Selection of the best Classification Features by Various Algorithms

Once the image objects have been created, among the several classifications features available in eCognition software, the best subsets were selected through ACO, GR, PSO, RF, GA, and CFS methods. The best features subset selection aimed to distinguish the landslide objects from non-landslide objects with high classification accuracy. The number of features in a subset to be selected was set to be lower than the number of samples in the landslide inventory map to avoid overfitting and reduce model complexity (Yu *et al*., 2006).

Overall, in order to detect the landslide locations 82 features were Mean and StdDev (Intensity, DEM, DSM, Slope, Aspect, Height), texture information All directions,0o,45o,90o,135o (Gray-level co-occurrence matrix (GLCM) correlation, GLCM Dissimilarity, GLCM angular second moment, GLCM StdDev, GLCM Mean, GLCM Contrast, GLCM Entropy, GLCM Homogeneity, GLDV angular second moment, Grey level difference vector (GLDV) Mean, GLDV Entropy and GLDV Contrast) and Mean and StdDev (Red, Green and Blue, Max. diff, and Brightness). The values of these features are expressed in mean and standard deviation (StdDev). Many the features were initially removed from the analysis due to the landslide class of the study area and only those that have the possibility of transferability were selected. The six feature selection algorithms selected the same features but provided different ranks (i.e. combination) and subsequently yield different landslide detection accuracy (Table 1).

The RF and SVM model were used in evaluation the process, and the inventory map was divided into training (70%) and testing (30%) sets. The values of their parameters should be placed in other to apply the six feature selection methods. In accordance with the

Table 1. Multi- resolution segmentation parameters

No.	Initial parameters			Iteration (Optimal parameters)		
	Scale	Shape	Compactness	Scale	Shape	Compactness
1	30	0.3	0.5	65.37	0.34	0.58
2	50	0.1	0.1	75.52	0.40	0.50
3	80	0.1	0.1	100.00	0.45	0.74

preliminary analysis and previous studies (Sameen *et al*., 2017; Chen *et al*., 2016; Li *et al*., 2016; Duo *et al*., 2015; Karegowda *et al*., 2010; Kumar *et al*., 2006), these parameters were selected and are found to be suitable for this research. Results of ACO, GR, PSO, RF, GA, and CFS approaches with 70% of the inventory data were evaluated according to the overall accuracy (Table 2). The highest landslide detection accuracy (91.00%) was achieved by using the features selected by CFS trained and evaluated with RF and SVM models. Furthermore, the algorithms ACO and RF indicate better performance than the GR and PSO methods in both models (RF and SVM). This implies that large number of features does not signifies accurate in the landslide inventory map. It was also observed that the ideal number of features is 11 among 82

Table 2. Optimal features selection for detecting landslide using various algorithms

Algorithm	Optimal Feature	Accuracy (%)		Algorithm	Optimal Feature	Accuracy (%)	
		RF	SVM			RF	SVM
CFS	StdDe DTM	91.00	87.34	RF	GLCM Angular Second Moment	89.51	84.69
	GLCM Homogeneity				StdDev Intensity		
	Mean Slope				Mean Slope		
	GLCM Angular Second Moment				GLCM Homogeneity		
	Mean Intensity				StdDev Height		
	Mean Red				StdDe DTM		
	Mean DTM				Brightness		
	GLCM Contrast				StdDev Blue		
	GLCM Dissimilarity				GLCM Correlation		
	Brightness				StdDev DSM		
	StdDev Blue				GLCM Dissimilarity		
GR	StdDev Intensity	79.43	78.37	ACO	StdDev Intensity	90.68	85.77
	Mean Slope				GLCM Homogeneity		
	StdDev DSM				GLCM Angular Second Moment		
	GLCM Homogeneity				Mean Slope		
	StdDev Green				StdDev Height		
	StdDe DTM				Mean DTM		
	GLCM Angular Second Moment				GLCM StdDe		
	StdDev Red				Mean Red		
	GLCM Contrast				StdDev Height		
	Brightness				StdDe DTM		
	GLCM DSM				GLCM StdDe		
PSO	Mean Slope	79.66	80.44	GA	GLCM Dissimilarity	79.61	78.39
	StdDe DTM				GLCM Angular Second Moment		
	Mean Intensity				StdDev Intensity		
	StdDev Green				Mean Slope		
	GLCM Angular Second Moment				GLCM Homogeneity		
	Mean DTM				GLCM Correlation		
	GLCM Correlation				StdDe Blue		
	Mean Red				Mean Red		
	StdDev Height				StdDev Green		
	GLCM Contrast				StdDe DTM		
	Brightness				Brightness		

available features (see Table 2).

Table 2 showed that several features, such as the StdDe DTM and GLCM Homogeneity were found to be the most important features for distinguishing landslide objects from other objects in the scene. In addition, based on the results of other feature selection methods, the most important features were slope and texture information represented in GLCM Homogeneity, GLCM correlation, and GLCM angular second moment.

The effect of the number of iterations on feature selection was also analyzed. Table 2 shows the 11 features selected in each iteration by using six methods. This experiment was executed for the best subset (11 features) and high accuracy was achieved. Different features were selected as optimum in each iteration. The result indicates that the same classification accuracy can be achieved with different feature combinations. Therefore, it is not sufficient to select only the significant features, combination of features should be selected as implemented in this study.

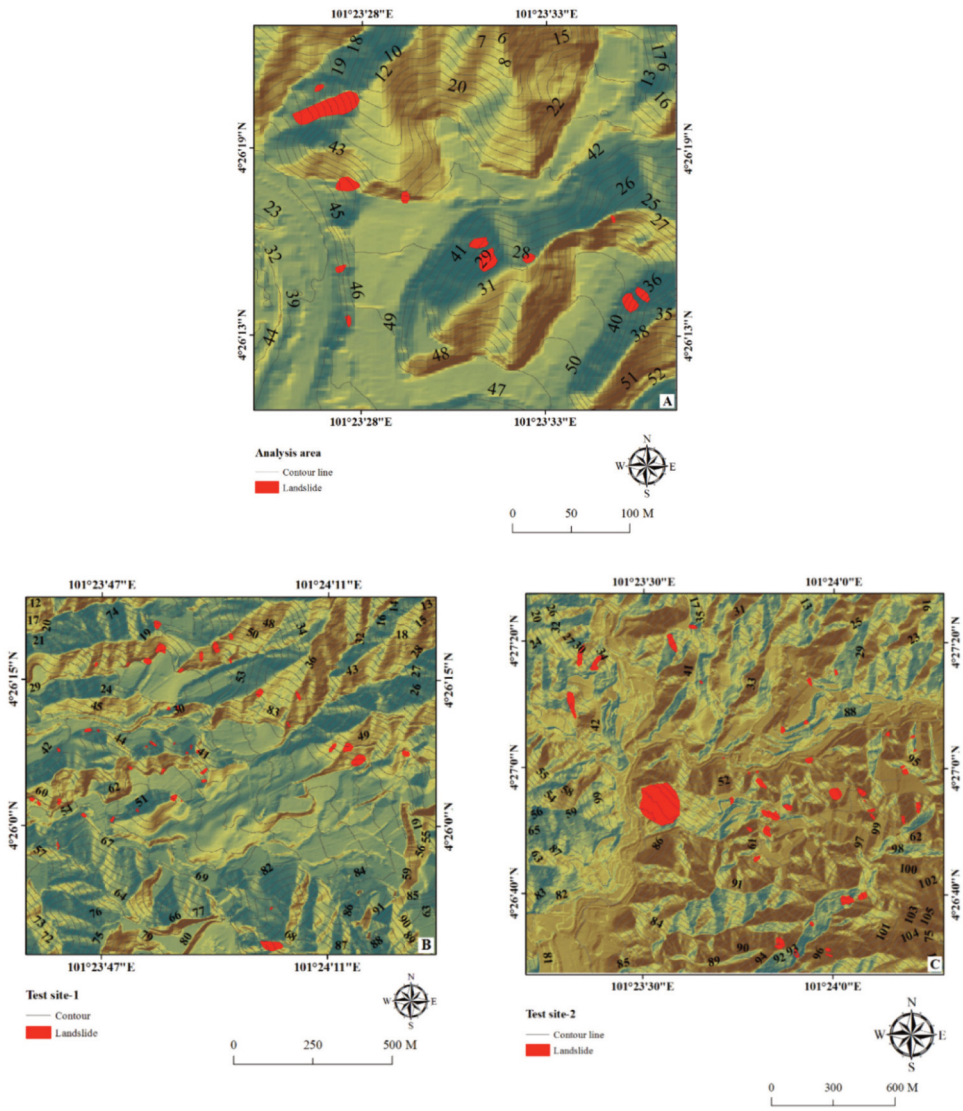

Fig. 6. Shows the results of support vector machine (A) analysis area (B) Test sit-1 (C) Test sit-2.

3) Results of the SVM and RF Models

First, the 70% training set was used to train the SVM model on the analysis area, site-1, and site-2. When all the features were utilized, the qualitative assessment results were poor. Furthermore, the quantitative assessment showed that the overall accuracies of the results were 74.73%, 71.09%, and 66.57% for the study area, site-1, and site-2, respectively. On the contrary, the SVM model that used the optimal features generated high-quality results in the qualitative assessment and performed accurate identification of the locations of landslides. The quantitative assessment demonstrated that the overall accuracy of the SVM model using the optimal features was 87.34% for the analysis area, as shown in Fig. 6. Fig. 6 also shows that the classification results for site-1 and site-2 achieved overall accuracies of 86.82% and 84%, respectively.

The results of the qualitative assessment of the RF model were of poor quality. The overall accuracies in the quantitative assessment were 77%, 72.83%, and 68.78% for the analysis area, site-1, and site-2,

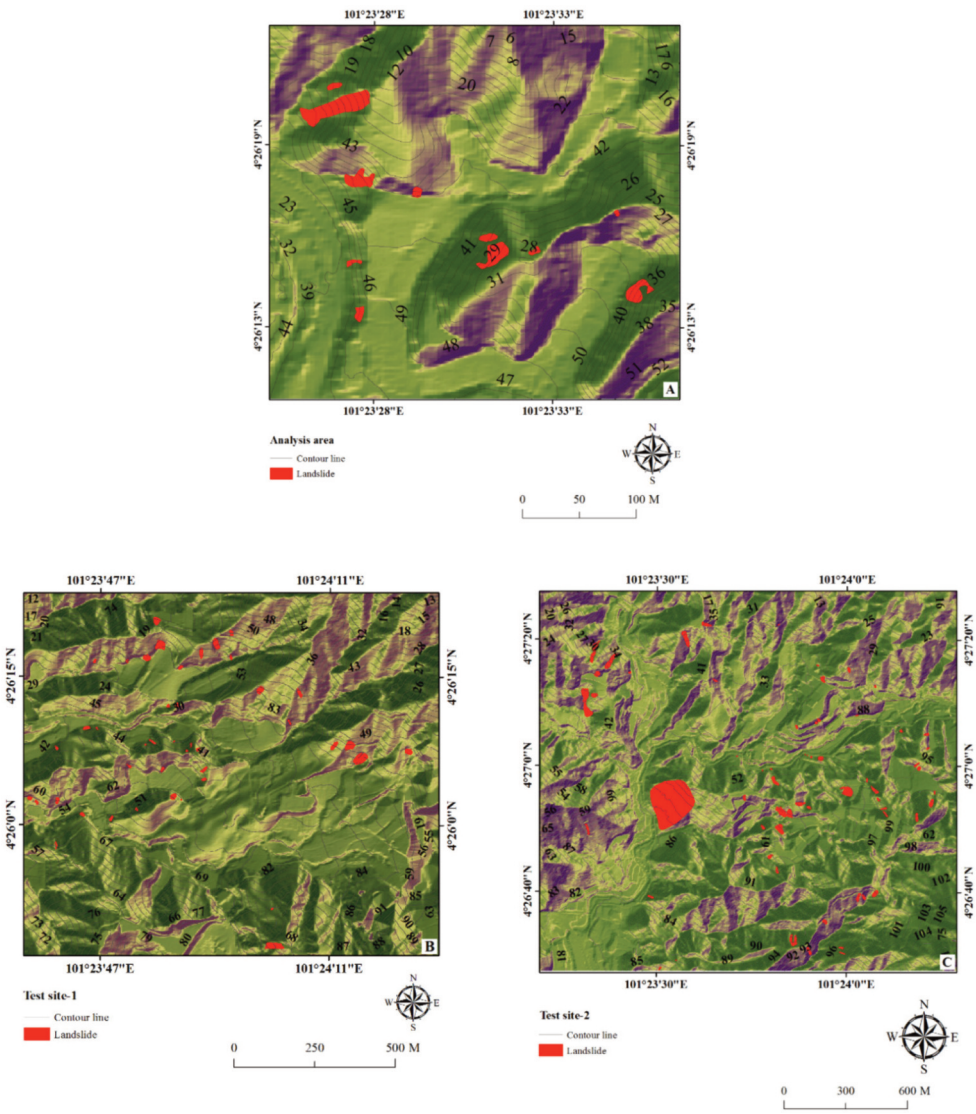

Fig. 7. Shows the results of random forest (A) analysis area (B) Test sit-1 (C) Test sit-2.

respectively. These results were obtained when the 70% of the training set and all the features were used to train the RF classifier. When the same training set ratio (i.e., the 70% of the training dataset) and only the optimal features were used, the RF model produced high-quality results and accurately identified landslide locations in the qualitative assessment. In the quantitative assessment of the analysis area, the overall accuracy and kappa coefficient were 91% and 0.84, respectively (Fig. 7). Fig. 7 Shows that the classification results for site-1 and site-2 achieved overall accuracies of 88.68% and 86%, respectively.

The results of the RF and SVM models demonstrated that using the six algorithms in feature selection and applying the optimized segmentation parameters with the use of high-resolution LiDAR, orthophotos, and texture information enhanced the models performance and improved the transferability of the RF and SVM models.

4) Transferability of Models

The training samples were evaluated using a stratified random sampling method. The 70% of training set was applied to train the RF and SVM

Table 3. Results comparison based on Overall accuracy and Kappa coefficient for important features and full features using RF and SVM algorithms

Area	Feature	Algorithms	Overall Accuracy %	Kappa Accuracy %
Analysis area	Full feature	RF	77.00	0.69
Test sit-1			72.83	0.67
Test sit-2			68.78	0.69
Analysis area	Optimal selected features		91.00	0.84
Test sit-1			88.68	0.81
Test sit-2			86.00	0.76
Analysis area	Full feature	SVM	74.73	0.66
Test sit-1			71.09	0.62
Test sit-2			66.57	0.68
Analysis area	Optimal selected features		87.34	0.81
Test sit-1			86.82	0.73
Test sit-2			84.00	0.76

Table 4. Results comparison based on User's Accuracy and Producer's Accuracy for important features and full features using RF and SVM algorithms

Area	Feature	Algorithms	User's Accuracy %	Producer's Accuracy %
Analysis area	Full feature	RF	72.21	74.34
Test sit-1			70.34	72.89
Test sit-2			69.55	71.54
Analysis area	GFS selected features		80.68	79.88
Test sit-1			76.57	78.17
Test sit-2			74.45	76.71
Analysis area	Full feature	SVM	70.19	71.05
Test sit-1			65.08	67.86
Test sit-2			63.37	66.56
Analysis area	GFS selected features		78.78	79.11
Test sit-1			75.23	77.69
Test sit-2			73.44	75.62

models with either all features or only the optimal features. When the RF and SVM models using all the features were applied, overall accuracies of 77% and 74% were achieved, respectively (Table 4). As shown in Table 3, the overall accuracies of the RF model (SVM model) for site-1 and site-2 were 72.83% (71.09%) and 68.78% (66.57%), respectively. When RF and SVM models using only the optimal features were used for the analysis area, the overall accuracies of the results were 91% and 87.34%, respectively. The overall accuracies for site-1 and site-2 of the RF model (SVM model) were 88.68% (86.82%) and 86% (84%), respectively (Table 3).

Table 4 shows the results of the user's and producer's accuracies of the RF and SVM classifiers using either only the optimal features or all features for the analysis area, site-1, and site-2. The results showed that the RF classifier exhibited higher accuracies for all the mentioned areas.

5) Evaluation via Precision/Recall method

One of the well-known methods for quantitative counting accuracy assessment is Precision/Recall method. The proposed method was evaluated using field observation for each block (Nyland, 1996) (see Eq. 18, Eq. 19 and Eq. 20).

$$\text{Precision} = \frac{TP}{TP + FP} \tag{18}$$

$$\text{Recall} = \frac{TP}{TP + FN} \tag{19}$$

$$\text{F} - \text{measure} = \frac{(1 + \alpha) \times \text{Precision} \times \text{Recall}}{\alpha \times \text{Precision} + \text{Recall}} \tag{20}$$

where a True Positive (TP) is the number of correctly detected landslide. A False Negative (FN) is a landslide that is not detected. A False Positive (FP) shows a pixel that is recognized as a landslide but it is something else. The α is a non-negative scalar. In this study, α is set to 0.5 as suggested in Lin *et al*. (2011). Also, the success rate can be computed using another equation which is to determine the positive counted rate by dividing segmented numbers with total trees.

Table 5 displays the results of the proposed method, which achieved very high accuracy assessment in all studies. This demonstrates that the proposed method can be transferrable to another spatial dataset with the same climate and condition.

In this current study, the accuracy assessments also were performed in two categories of quantitative and qualitative to measure the precision of applied methods. Precision/Recall method was applied for measuring the accuracy of landslide detection quantitatively. The actual number of landslide events were collected via field surveying as a reference. Then, the results of RF and SVM models were compared to landslide inventory. The landslides would be counted as a corrected detection, as long as it is recognized in segments by weather bigger size of segment border or smaller. The key point in landslide counting is having even a single segment on occurred landslide and area of landslides are not considerable in mentioned

TABLE 5. Performance evaluation of RF and SVM Models.

Methods	Analysis Area		Test site-1		Test site-2	
	RF	SVM	RF	SVM	RF	SVM
Real inventory	13	13	43	43	64	64
TP	11	10	42	40	62	60
FN	2	3	1	3	2	4
FP	1	1	4	7	5	9
Precision	0.917	0.909	0.913	0.851	0.925	0.870
Recall	0.846	0.769	0.977	0.930	0.969	0.938
F-measure	0.892	0.857	0.933	0.876	0.939	0.891

assessment.

F-measure stands for overall accuracy in counting landslide detection, showed a consistence result in analysis area and tested areas (i.e. Test site-1 and 2) for two models (i.e. RF and SVM). RF however, exhibited the highest results for landslide detection in all aforementioned areas as illustrated in Table 5. While, SVM achieved low accuracy in detecting the landslide (see Table 5). Thus, based on the assessed accuracy measurements proposed methodology improve the landslide detection analysis quantitatively and qualitatively.

5. Discussion

This research uses six feature selection methods, object-based technique and LiDAR data to improve the accuracy of landslide inventory mapping. It was sufficient to optimize segmentation parameters like scale, shape, and compactness using FbSP optimizer in delineating landslide boundaries. Because, optimized segmentation parameters facilitate the generation of accurate objects segment and uses spatial and texture features to distinguish another land cover classes and reduces the influence of under and over segmentation. Since landslides can be classified according to their features, accurate segmentation is essential for differentiating between the classes. Even though segmentation results could prove difficult sometimes due to shape of objects, optimization approaches can be used to improve its accuracy (Pradhan and Mezaal, 2017). Among these methods, the selection of a subset with optimal features can significantly improve the results of classification because nonsignificant features could have redundant information and subsequently degrade classification accuracy.

On the basis of the results of the RF and SVM classifiers, three of algorithms, namely, CFS, ACO, and RF, exhibited the highest ranks in landslide detection, respectively. The results of CFS showed the high classification accuracy, it was a rapid and time effective method. Among all the compared feature selection algorithms, ACO is second powerful technique for selecting a subset from available features effectively. For the RF algorithm, the ranks of RF also illustrated the significance of subset features for enhancing the results of accuracy. These methods are easier as their mathematical operations can be solved with the primitive mathematical operators. They are cost effective as their application does not require high speed or memory. Moreover, their basic concept of these above-mentioned methods is simple that their ideas can be summarized in simple code which are made up of few lines.

The result indicated the importance of this step in detecting landslides in the OBIA framework. Using feature selection for object detection can reduce computational complexity, eliminate the irrelevant features, reduce the dependence on subjective expert knowledge, simplify of the developed rules, and improve the model. Distinguishing between landslides and other landcovers in densely vegetated terrains and hilly areas like Cameron Highlands (cut slope, bare soil and man-made slopes) could be quite challenging. Therefore, the transferability results of the feature selection form of the analysis area to the sites (site-1 and 2) were tested as presented in Fig. 6B, C and 7B, and C. It was observed that the location of landslides was separated by using the relevant feature as shown in Table 3. According to Stumpf *et al*. (2011), the overall accuracy of landslide detection applied to other areas could decrease even if the same method was used in the development of the model. This reduction in accuracy could be due to difference in landslide characteristics and environmental conditions. Also, spatial resolutions of images, differences in the sensors used, and illumination conditions could be contributed to the challenges reported recently (Rau *et al*., 2014).

In this context, landslide detection techniques are

appropriate for generating a well-organized landslide inventory map that is useful for qualitative/quantitative hazard assessment. Various methods for landslide mapping have been proposed; however, no method has effectively revealed the ideal results. Li *et al*. (2015) identified landslide by using LiDAR data, object based image analysis and random forest. The overall accuracy of their study was 89%. Dou *et al*. (2015) integrated object-based approach and a Genetic Algorithm (GA) algorithm with help of LiDAR data for landslide detection. The quantitative assessment of showed that the overall accuracy of their study was 87%. The reasons are that LiDAR intensity data was not involved in their work and not all spectral and spatial information of object because unfitting delineation of the segmentation for landslide object. Therefore, many misclassifications can be seen in the results.

It is absolutely necessary to take the required measures in other to avoid landslide separation from the most similar land cover classes (i.e. man-made, bare soil and cut slope). The morphological characteristics of landslide map differs. For instance, slope, the shape, and other characteristics such as dip direction, texture, width and length of the surface terrain could change after landslide. Therefore, by using relevant features derived from very high resolution LiDAR data and texture and geometric features can be used to distinguish between landslides and bare soil. In addition, applying different optimization techniques helped us to improve the classification accuracy in landslide detection over other landcover classes, such as bare land, cut slope, etc., as described previously by Pradhan and Mezaal(2017). Their results demonstrated that using optimized techniques with very high resolution LiDAR data enabled them to separate landslide from other types of land cover. Furthermore, Mezaal *et al*. (2017a) suggested that using the object feature from LiDAR data is suitable for resolving landslide identification issues.

6. Validation

The reliability of the proposed method was further validated by conducting a field investigation. A handheld GPS device (GeoExplorer 6000) was utilized to identify landslide locations, as shown in Fig. 8. A more detailed information like source area, direction, run out, volume and deposition was obtained from in-situ measurements which proves the reliability of the inventory map produced in the field using GeoExplorer 6000 handheld GPS. All the information obtained from the field measurements allowed for the assessment of the precision and reliability of the produced landslide inventory map. The field investigation confirmed that the landslides detected using the proposed method was accurate. Thus, the proposed method can identify landslide locations and produce a credible landslide inventory map for the Cameron Highlands in Malaysia.

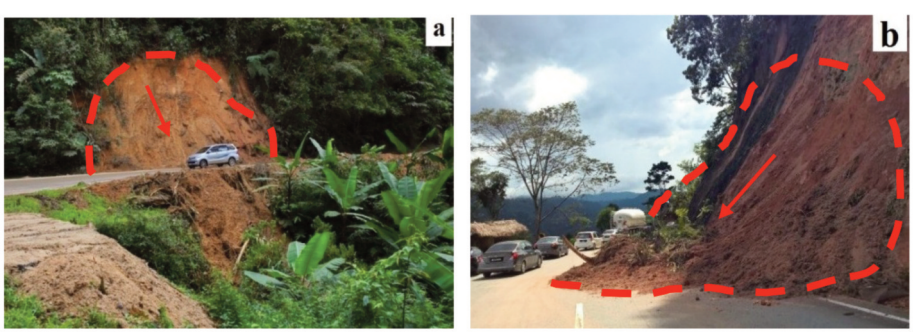

Fig. 8. Landslides locations in the study area; (a) Taman Mawar, Kuala Terla and (b) Jalan Tapah-Ringlet.

7. Conclusion

This study indicated the importance of using the optimized parameters of multiresolution segmentation to achieve the highest overall accuracy, as they allow for the accurate delineation of landslide boundaries. The RF results model were much more accurate than the results of SVM model when either all features or only the optimal features were used.

The quantitative assessment revealed that the overall accuracy of the RF model and (SVM model) using the optimal features were 91% and (87.34%) for the analysis area, while, the results for site-1 and site-2 achieved overall accuracies of 88.68% and 86%, (86.82%) and (84%), respectively. Moreover, the results of transferability model showed that, RF and SVM models were used for the analysis area, the overall accuracies of the results were 91% and 87.34%, respectively. The overall accuracies of RF model (SVM model) were 88.68% (86.82%) and 86% (84%), for site-1 and site-2 of the, respectively.

The algorithm with the highest ranks in feature selection for landslide detection were CFS, ACO and RF. The feature selection algorithm reduced the dimensionality of the object features, expedited the training of RF and SVM classifies, and improved the classification accuracy of these classifiers. The SVM classifier was more sensitive to the feature selection than the RF classifier. In addition, field investigation was applied for performing the second round of validation. Therefore, the proposed method is suitable for the accurate identification of landslide locations and production of reliable inventory maps, which are crucial to avoid disasters in urban areas. The results indicate that the significance of the relevant selection achieved from very high-resolution airborne laser scanning data, visible bands, texture features for improve the detecting of the locations of landslide. Overall, using various feature selection algorithms and a supervised approach based on RF and SVM models yielded robust results and increased the efficiency and cost effectiveness of the development of landslide inventory maps with the use of high-resolution LiDAR-derived data, orthophotos, and texture information.

References

Aladesote, I., A. Olutola, and O. Olayemi, 2016. Feature or Feature Extraction for Intrusion Detection System using Gain Ratio and Principal Component Analysis (PCA), *Methodology*, 4(3).

Alwan, H. B. and K. R. Ku-Mahamud, 2012. Optimizing support vector machine parameters using continuous ant colony optimization, *2012 7th International Conference on Computing and Convergence Technology (ICCCT)*, Dec. 3-5, Seoul, South Korea, pp. 164-169.

Anders, N.S., A.C. Seijmonsbergen, and W. Bouten, 2011. Segmentation optimization and stratified object-based analysis for semi-automated geomorphological mapping, *Remote Sensing of Environment*, 115(12): 2976-2985.

Antonini, G., F. Ardizzone, M. Cardinali, M. Galli, F. Guzzetti, and P. Reichenbach, 2002. Surface deposits and landslide inventory map of the area affected by the 1997 Umbria-Marche earthquakes, *Bollettino Della Societá Geologica Italiana*, 121(1): 843-853.

Ardizzone, F., M. Cardinali, M. Galli, F. Guzzetti, and P. Reichenbach, 2007. Identification and mapping of recent rainfall-induced landslides using elevation data collected by airborne Lidar, *Natural Hazards and Earth System Science*, 7(6): 637-650.

Barbarella, M., M. Fiani, and A. Lugli, 2013. Application of LiDAR-derived DEM for detection of mass movements on a landslide,

International Archives of the Photogrammetry, *Remote Sensing and Spatial Information Sciences*, 1(3): 89-98.

Belgiu, M. and L. Drăguţ, 2014. Comparing supervised and unsupervised multiresolution segmentation approaches for extracting buildings from very high resolution imagery, *ISPRS Journal of Photogrammetry and Remote Sensing*, 96: 67-75.

Benz, U. C., P. Hofmann, G. Willhauck, I. Lingenfelder, and M. Heynen, 2004. Multi-resolution, object-oriented fuzzy analysis of remote sensing data for GIS-ready information, *ISPRS Journal of Photogrammetry and Remote Sensing*, 58(3): 239-258.

Blaschke, T., 2010. Object based image analysis for remote sensing, *ISPRS Journal of Photogrammetry and Remote Sensing*, 65(1): 2-16.

Booth, A.M., J. J. Roering, and J. T. Perron, 2009. Automated landslide mapping using spectral analysis and high-resolution topographic data: Puget Sound lowlands, Washington, and Portland Hills, Oregon, *Geomorphology*, 109(3-4): 132-147.

Borghuis, A., K. Chang, and H. Lee, 2007. Comparison between automated and manual mapping of typhoon triggered landslides from SPOT-5 imagery, *International Journal of Remote Sensing*, 28(8): 1843-1856.

Borkowski, A., Z. Perski, T. Wojciechowski, G. Jóźków, and A. Wojcik, 2011. Landslides mapping in Roznow Lake vicinity, Poland using airborne laser scanning data, *Acta Geodyn. Geomater*, 8(3): 163.

Brardinoni, F., O. Slaymaker, and M.A. Hassan, 2003. Landslide inventory in a rugged forested watershed: a comparison between air-photo and field survey data, *Geomorphology*, 54(3): 179-196.

Breiman, L., 2001. Random forests, *Machine Learning*, 45(1): 5-32.

Bui, D.T., B. Pradhan, O. Lofman, I. Revhaug, and O.B. Dick, 2012. Landslide susceptibility mapping at Hoa Binh province (Vietnam) using an adaptive neuro-fuzzy inference system and GIS, *Computers & Geosciences*, 45: 199-211.

Cao, L. Y. and L. Z. Xia, 2007. An ant colony optimization approach for SAR image segmentation, *2007 International Conference on Wavelet Analysis and Pattern Recognition (ICWAPR)*, Beijing, China, Nov. 2-4, vol. 1, pp. 296-300.

Chen, Q., Y. Chen, and W. Jiang, 2016. Genetic Particle Swarm Optimization–Based Feature Selection for Very-High-Resolution Remotely Sensed Imagery Object Change Detection, *Sensors*, 16(8): 1204.

Chen, W., X. Li, Y. Wang, G. Chen, and S. Liu, 2014. Forested landslide detection using LiDAR data and the random forest algorithm: A case study of the Three Gorges, China, *Remote Sensing of Environment*, 152: 291-301.

Chen, T., J.C. Trinder, and R. Niu, 2017. Object-Oriented Landslide Mapping Using ZY-3 Satellite Imagery, Random Forest and Mathematical Morphology for the Three-Gorges Reservoir, China, *Remote Sensing*, 9(4): 333.

Dadaneh, B.Z., H. Y. Markid, and A. Zakerolhosseini, 2016. Unsupervised probabilistic feature selection using ant colony optimization, *Expert Systems with Applications*, 53: 27-42.

Danneels, G., E. Pirard, and H.B. Havenith, 2007. Automatic landslide detection from remote sensing images using supervised classification methods, *Proc. of 2007 IEEE International Geoscience & Remote Sensing Symposium*, Barcelona, Jul.23-28, pp. 3014-3017.

De Blasio, F.V., 2011. Landslides in Valles Marineris

(Mars): a possible role of basal lubrication by sub-surface ice, *Planetary and Space Science*, 59(13): 1384 1392.

Definiens, A.G., 2007. *Definiens developer 7 reference book*, Definiens AG, München, pp. 21-24.

R Development Core Team, 2010. R: A language and environment for statistical computing, *R Foundation for Statistical Computing Vienna, Austria, ISBN 3-900051-07-0, URL: http:// www.R-project. org*.

Dorigo, M. and T. Stützle, 2010. Ant colony optimization: overview and recent advances, In *Handbook of metaheuristics*, pp. 227-263, Springer, US.

Dou, J., K.-T. Chang, S. Chen, A.P. Yunus, J.K. Liu, H. Xia, and Z. Zhu, 2015. Automatic case-based reasoning approach for landslide detection: integration of object-oriented image analysis and a genetic algorithm, *Remote Sensing*, 7(4): 4318-4342.

Drăguţ, L. and T. Blaschke, 2006. Automated classification of landform elements using object-based image analysis, *Geomorphology*, 81(3): 330-344.

Drăguţ, L., D. Tiede, and S.R. Levick, 2010. A tool to estimate scale parameter for multiresolution image segmentation of remotely sensed data, International *Journal of Geographical Information Science*, 24(6): 859-871.

Duro, D.C., S.E. Franklin, and M.G. Dubé, 2012. Multi-scale object-based image analysis and feature selection of multi-sensor earth observation imagery using random forests, *International Journal of Remote Sensing*, 33(14): 4502-4526.

Fassnacht, F.E., F. Hartig, H. Latifi, C. Berger, J. Hernández, P. Corvalán, and B. Koch, 2014. Importance of sample size: data type and prediction method for remote sensing-based estimations of aboveground forest biomass, *Remote Sensing of Eenviroment*, 154: 102-114.

Fei, L.Y. and Y.L. Lee, 2009. The rapid method to identify landslide areas and disasters triggered by Typhoon Morakot, *Sino-Geotechnics*, 122: 61-68.

Fiorucci, F., M. Cardinali, R. Carlá, M. Rossi, A. Mondini, L. Santurri, and F. Guzzetti, 2011. Seasonal landslide mapping and estimation of landslide mobilization rates using aerial and satellite images, *Geomorphology*, 129(1): 59-70.

Foody, G. M. and A. Mathur, 2006. The use of small training sets containing mixed pixels for accurate hard image classification: Training on mixed spectral responses for classification by a SVM, *Remote Sensing of Environment*, 103(2): 179-189.

Galli, M., F. Ardizzone, M. Cardinali, F. Guzzetti, and P. Reichenbach, 2008. Comparing landslide inventory maps, *Geomorphology*, 94(3): 268-289.

Gao, Y. and J. F. Mas, 2008. A comparison of the performance of pixel-based and object-based classifications over images with various spatial resolutions, *Online Journal of Earth Sciences*, 2(1): 27-35.

Goldberg, D., 1989. *Genetic Algorithms in Search, Optimization and Machine Learning*, Addison-Wesley, Boston, MA, USA.Grimm, R., T. Behrens, M. Märker, and H. Elsenbeer, 2008. Soil organic carbon concentrations and stocks on Barro Colorado Island digital soil mapping using Random Forests analysis, *Geoderma*, 146(1-2): 102-113.

Guzzetti, F., A. C. Mondini, M. Cardinali, F. Fiorucci, M. Santangelo, and K.-T. Chang, 2012. Landslide inventory maps: New tools for an old problem, *Earth-Science Reviews*, 112(1): 42-66.

Guzzetti, F., P. Reichenbach, M. Csardinali, M. Galli, and F. Ardizzone, 2005. Probabilistic landslide hazard assessment at the basin scale, *Geomorphology*, 72 (1): 272-299.

Han, J., J. Pei, and M. Kamber, 2011. *Data Mining: Concepts and Techniques*, Elsevier, Amsterdam, Netherlands.

Heleno, S., M. Matias, P. Pina, and A.J. Sousa, 2015. Automated object-based classification of rain-induced landslides with VHR multispectral images in Madeira Island, *Natural Hazards & Earth System Sciences Discussions*, 3(9).

Heleno, S., M. Matias, P. Pina, and A. J. Sousa, 2016. Semiautomated object-based classification of rain-induced landslides with VHR multispectral images on Madeira Island, *Natural Hazards and Earth System Sciences*, 16: 1035-1048.

Imani, M.B., T. Pourhabibi, M.R. Keyvanpour, and R. Azmi, 2012. A New Feature Selection Method Based on Ant Colony and Genetic Algorithm on Persian Font Recognition, *International Journal of Machine Learning and Computing*, 2(3): 278.

Jebur, M.N., B. Pradhan, and M.S. Tehrany, 2014. Detection of vertical slope movement in highly vegetated tropical area of Gunung pass landslide, Malaysia, using L-band InSAR technique, *Geosciences Journal*, 18(1): 61-68.

Karegowda, A.G., M. Jayaram, and A. Manjunath, 2010. Feature subset selection problem using wrapper approach in supervised learning, *International Journal of Computer Applications*, 1(7): 13-17.

Karegowda, A.G., A. Manjunath, and M. Jayaram, 2010. Comparative study of feature selection using gain ratio and correlation based feature selection, *International Journal of Information Technology and Knowledge Management*, 2(2): 271-277.

Kursa, M.B. and W.R. Rudnicki, 2010. Feature selection with the Boruta package, *Journal of Statistical Software*, 36(11): 1-13.

Ladha, L. and T. Deepa, 2011. Feature selection methods and algorithms, *International Journal on Computer Science and Engineering*, 1(3): 1787-1797.

Lee, S., K.Y. Song, H.J. Oh, and J. Choi, 2012. Detection of landslides using web-based aerial photographs and landslide susceptibility mapping using geospatial analysis, *International Journal of Remote Sensing*, 33(16): 4937-4966.

Li, L. L. and J. K. Wang, 2012. SAR image ship detection based on ant colony optimization, *2012 5th International Congress on Image and Signal Processing (CISP)*, Chongqing, China, Oct. 16-18, pp. 1100-1103.

Li, M., L. Ma, T. Blaschke, L. Cheng, and D. Tiede, 2016. A systematic comparison of different object-based classification techniques using high spatial resolution imagery in agricultural environments, *International Journal of Applied Earth Observation and Geoinformation*, 49: 87-98.

Li, X., X. Cheng, W. Chen, G. Chen, and S. Liu, 2015. Identification of forested landslides using LiDar data, object-based image analysis, and machine learning algorithms, *Remote Sensing*, 7(8): 9705-9726.

Liaw, A. and M. Wiener, 2002. Classification and regression by random Forest, *R news*, 2(3): 18-22.

Lin, C.W., C.M. Tseng, Y.H. Tseng, L.Y. Fei, Y.C. Hsieh, and P. Tarolli, 2013. Recognition of large scale deep-seated landslides in forest areas of Taiwan using high resolution topography, *Journal of Asian Earth Sciences*, 62: 389-400.

Liu, T., Z. Yuan, J. Sun, J. Wang, N. Zheng, X. Tang, H. Y. Shum, 2011. Learning to detect a salient object, *IEEE Transactions on Pattern Analysis and Machine Intelligence*, 33(2): 353-367.

Lippitt, C.D., J. Rogan, Z. Li, J.R. Eastman, and T.G. Jones, 2008. Mapping Selective Logging in Mixed Deciduous Forest, *Photogrammetric Engineering & Remote Sensing*, 74(10):

1201-1211.

Lu, G. Y. and D. W. Wong, 2008. An adaptive inverse-distance weighting spatial interpolation technique, *Computers and Geosciences*, 34(9): 1044-1055.

Lu, P., A. Stumpf, N. Kerle, and N. Casagli, 2011. Object-oriented change detection for landslide rapid mapping, *IEEE Geoscience and Remote Sensing Letters*, 8(4): 701-705.

Ma, H.R., X. Cheng, L. Chen, H. Zhang, and H. Xiong, 2016. Automatic identification of shallow landslides based on Worldview2 remote sensing images, *Journal of Applied Remote Sensing*, 10(1): 016008-016008.

Malamud, B.D., D.L. Turcotte, F. Guzzetti, and P. Reichenbach, 2004. Landslide inventories and their statistical properties, *Earth Surface Processes and Landforms*, 29(6): 687-711.

Martha, T.R., N. Kerle, C.J. Van Westen, V. Jetten, and K.V. Kumar, 2011. Segment optimization and data-driven thresholding for knowledge-based landslide detection by object-based image analysis, *IEEE Transactions on Geoscience and Remote Sensing*, 49(12): 4928-4943.

McKean, J. and J. Roering, 2004. Objective landslide detection and surface morphology mapping using high-resolution airborne laser altimetry, *Geomorphology*, 57(3): 331-351.

Meyer, D., E. Dimitriadou, K. Hornik, A. Weingessel, and F. Leisch, 2014. *e1071: Misc Functions of the Department of Statistics (e1071)*, R Package Version 1.6-4, TU Wien, Vienna.

Mezaal, M.R., B. Pradhan, M.I. Sameen, H.Z. Shafri, and Z.M. Yusoff, 2017a. Optimized Neural Architecture for Automatic Landslide Detection from High Resolution Airborne Laser Scanning Data, *Applied Sciences*, 7(7): 730.

Mezaal, M. R., B. Pradhan, H. Z. M. Shafri, and Z. M. Yusoff, 2017b. Automatic landslide detection using Dempster–Shafer theory from LiDAR-derived data and orthophotos, *Geomatics, Natural Hazards and Risk*, 1-20.

Miller, P.E., J.P. Mills, S.L. Barr, S.J. Birkinshaw, A. J. Hardy, G. Parkin, and S.J. Hall, 2012. A remote sensing approach for landslide hazard assessment on engineered slopes, *IEEE Transactions on Geoscience and Remote Sensing*, 50(4): 1048-1056.

Miner, A.S., P. Flentje, C. Mazengarb, and D.J. Windle, 2010. Landslide Recognition using LiDAR derived Digital Elevation Models-Lessons learnt from selected Australian examples.

Moine, M., A. Puissant, and J.P. Malet, 2009. Detection of landslides from aerial and satellite images with a semi-automatic method. Application to the Barcelonnette basin (Alpes-de-Hautes-Provence, France), *In Landslide processes-from geomorphologic mapping to dynamic modelling*, pp. 63-68.

Mutanga, O., E. Adam, and M.A. Cho, 2012. High density biomass estimation for wetland vegetation using WorldView-2 imagery and random forest regression algorithm, *International Journal of Applied Earth Observation and Geoinformation*, 18: 399-406.

Nichol, J. E., A. Shaker, and M. S. Wong, 2006. Application of high-resolution stereo satellite images to detailed landslide hazard assessment, *Geomorphology*, 76(1): 68-75.

Nyland, R. D., 2016. *Silviculture: concepts and applications*, Waveland Press, Long Grove, IL, USA.

Olaya, V., 2009. Basic land-surface parameters, *Developments in Soil Science*, 33: 141-169.

Pal, M. and G. M. Foody, 2010. Feature selection for classification of hyperspectral data by SVM, *IEEE Transactions on Geoscience and Remote Sensing*, 48(5): 2297-2307.

Pal, M., P.M. Mather, 2003. An assessment of the effectiveness of decision tree methods for

land cover classification, *Remote Sensing of Environment*, 86(4): 554-565.

Parpinelli, R. S., H. S. Lopes, and A. A. Freitas, 2002. Data mining with an ant colony optimization algorithm, *IEEE Transactions on Evolutionary Computation*, 6(4): 321-332.

Pawłuszek, K. and A. Borkowski, 2016. Landslides identification using airborne laser scanning data derived topographic terrain attributes and support vector machine classification, The International Archives of the Photogrammetry, Remote Sensing and Spatial Information Sciences, XXIII ISPRS Congress, Prague, Czech Republic, Jul. 12-19, vol. XLI-B8.

Pedergnana, M., P. R. Marpu, M. Dalla Mura, J. A. Benediktsson, and L. Bruzzone, 2013. A novel technique for optimal feature selection in attribute profiles based on genetic algorithms, *IEEE Transactions on Geoscience and Remote Sensing*, 51(6): 3514-3528.

Pourghasemi, H.R., H.R. Moradi, S.F. Aghda, C. Gokceoglu, and B. Pradhan, 2014. GIS-based landslide susceptibility mapping with probabilistic likelihood ratio and spatial multi-criteria evaluation models (North of Tehran, Iran), *Arabian Journal of Geosciences*, 7(5): 1857-1878.

Pradhan, B., 2013. A comparative study on the predictive ability of the decision tree, support vector machine and neuro-fuzzy models in landslide susceptibility mapping using GIS, *Computers and Geosciences*, 51: 350-365.

Pradhan, B., M.N. Jebur, H.Z.M. Shafri, and M.S. Tehrany, 2016. Data Fusion Technique Using Wavelet Transform and Taguchi Methods for Automatic Landslide Detection From Airborne Laser Scanning Data and QuickBird Satellite Imagery, *IEEE Transactions on Geoscience and Remote Sensing*, 54(3): 1610-1622.

Pradhan, B. and S. Lee, 2010. Regional landslide susceptibility analysis using back-propagation neural network model at Cameron Highland, Malaysia, *Landslides*, 7(1): 13-30.

Pradhan, B. and M.R. Mezaal, 2017. Optimized Rule Sets for Automatic Landslide Characteristic Detection in a Highly Vegetated Forests, In *Laser Scanning Applications in Landslide Assessment*, pp. 51-68, Springer International Publishing AG, Cham, Switzerland.

Puissant, A., S. Rougier, and A. Stumpf, 2014. Object-oriented mapping of urban trees using Random Forest classifiers, *International Journal of Applied Earth Observation and Geoinformation*, 26: 235-245.

Rau, J.Y., K.T. Chang, Y.C. Shao, and C.C. Lau, 2012. Semi-automatic shallow landslide detection by the integration of airborne imagery and laser scanning data, *Natural Hazards*, 61(2): 469-480.

Rodriguez-Galiano, V.F., B. Ghimire, J. Rogan, M. Chica-Olmo, and J.P. Rigol-Sanchez, 2012. An assessment of the effectiveness of a random forest classifier for land-cover classification, *ISPRS Journal of Photogrammetry and Remote Sensing*, 67: 93-104.

Saeys, Y., I. Inza, and P. Larrañaga, 2007. A review of feature selection techniques in bioinformatics, *Bioinformatics*, 23(19): 2507-2517.

Sameen, M. I. and B. Pradhan, 2017. A Two-Stage Optimization Strategy for Fuzzy Object-Based Analysis Using Airborne LiDAR and High-Resolution Orthophotos for Urban Road Extraction, *Journal of Sensors*, 6:1-17.

Sameen, M.I., B. Pradhan, H.Z. Shafri, M.R. Mezaal, and H. Bin Hamid, 2017. Integration of Ant Colony Optimization and Object-Based Analysis for LiDAR Data Classification, *IEEE Journal of Selected Topics in Applied Earth Observations and Remote Sensing*, 10(5): 2055-2066.

Sheikhpour, R., M. A. Sarram, and R. Sheikhpour, 2016. Particle swarm optimization for bandwidth

determination and feature selection of kernel density estimation based classifiers in diagnosis of breast cancer, *Applied Soft Computing*, 40: 113-131.

Siyahghalati, S., A.K. Saraf, B. Pradhan, M.N. Jebur, and M.S. Tehrany, 2016. Rule-based semi-automated approach for the detection of landslides induced by 18 September 2011 Sikkim, Himalaya, earthquake using IRS LISS3 satellite images, Geomatics, *Natural Hazards and Risk*, 7(1): 326-344.

Srivastava, N., G. E. Hinton, A. Krizhevsky, I. Sutskever, and R. Salakhutdinov, 2014. Dropout: a simple way to prevent neural networks from overfitting, *Journal of Machine Learning Research*, 15(1): 1929-1958.

Stumpf, A. and N. Kerle, 2011. Object-oriented mapping of landslides using Random Forests, *Remote Sensing of Environment*, 115(10): 2564-2577.

Tang, A. M., C. Quek, and G. S. Ng, 2005. GA-TSKfnn: Parameters tuning of fuzzy neural network using genetic algorithms, *Expert Systems with Applications*, 29(4): 769-781.

Tehrany, M.S., B. Pradhan, and M.N. Jebuv, 2014. A comparative assessment between object and pixel-based classification approaches for land use/land cover mapping using SPOT-5 imagery, *Geocarto International*, 29(4): 351-369.

Van Den Eeckhaut, M., J. Poesen, F. Gullentops, L. Vandekerckhove, and J. Hervás, 2011. Regional mapping and characterisation of old landslides in hilly regions using LiDAR-based imagery in Southern Flanders, *Quaternary Research*, 75(3): 721-733.

Van Den Eeckhaut, M., J. Poesen, G. Verstraeten, V. Vanacker, J. Moeyersons, J. Nyssen, and L. Van Beek, 2005. The effectiveness of hillshade maps and expert knowledge in mapping old deep-seated landslides, *Geomorphology*, 67(3): 351-363.

Van Westen, C.J., E. Castellanos, and S.L. Kuriakose, 2008. Spatial data for landslide susceptibility, hazard, and vulnerability assessment: an overview, *Engineering Geology*, 102(3): 112-131.

Venkateswaran, K., T.S. Shree, N. Kousika, and N. Kasthuri, 2016. Performance Analysis of GA and PSO based Feature Selection Techniques for Improving Classification Accuracy in Remote Sensing Images, *Indian Journal of Science and Technology*, 9(16).

Verikas, A., A. Gelzinis, and M. Bacauskiene, 2011. Mining data with random forests: A survey and results of new tests, *Pattern Recognition*, 44(2): 330-349.

Wang, G., J. Joyce, D. Phillips, R. Shrestha, and W. Carter, 2013. Delineating and defining the boundaries of an active landslide in the rainforest of Puerto Rico using a combination of airborne and terrestrial LIDAR data, *Landslides*, 10(4): 503-513.

Wills, C. and T. McCrink, 2002. Comparing landslide inventories: The map depends on the method, *Environmental & Engineering Geoscience*, 8(4): 279-293.

Xue, B., M. Zhang, and W. N. Browne, 2013. Particle swarm optimization for feature selection in classification: A multi-objective approach, *IEEE transactions on cybernetics*, 43(6): 1656-1671.

Yu, W., B. Wu, T. Huang, X. Li, K. Williams, and H. Zhao, 2006. Statistical methods in proteomics, In *Springer Handbook of Engineering Statistics*, pp. 623-638, Springer-Verlag, London.

Zhang, Y., T. Maxwell, H. Tong, and V. Dey, 2010. Development of a supervised software tool for automated determination of optimal segmentation parameters for ecognition, pp. 5-7, na.

Zhen, Z., L.J. Quackenbush, S.V. Stehman, and L. Zhang, 2013. Impact of training and validation

sample selection on classification accuracy and accuracy assessment when using reference polygons in object-based classification, *International Journal of Remote Sensing*, 34(19): 6914-6930.